Desalination and Water Treatment
www.deswater.com

doi: 10.5004/dwt.2020.26229

204 (2020) 10–21
November

Pareto-optimization of MSF-OT/TVC desalination plant using surface response methodology and genetic algorithm

Ahlem Sellami, Mongi Ben Ali*, Lakdar Kairouani

Université de Tunis El Manar, Ecole Nationale d'Ingénieurs de Tunis, Unité de Recherche Energétique et Environnement, Tunis Belvédère, BP 37, 1002, Tunisie, emails: mongibenali2000@yahoo.fr (M. Ben Ali), ahlem.sellami@yahoo.fr (A. Sellami), lakdar_kairouani@yahoo.fr (L. Kairouani)

Received 21 May 2019; Accepted 6 June 2020

ABSTRACT

This paper describes an optimization approach of a novel configuration of a once-through multi-stage flash (MSF-OT) desalination plant. The system integrates a thermal vapor compression (TVC) unit within the conventional MSF-OT configuration. Three objectives controlling the operating cost of the installation were considered. The first is to maximize plant capacity production. The second is to minimize thermal energy consumption. The third is to minimize the feed seawater flow rate, which reduces electrical energy and chemical additives consumption. Solving the multi-objective optimization problem, using solvers of MATLAB software, led to obtaining a large number of optimal operating parameters of the MSF-OT/TVC plant. The comparison between the current operating state of the desalting installation using the MSF-OT process, and optimal operating states of the studied installation, showed a significant improvement in parameters controlling the operating cost of the installation. This improvement corresponded to a reduction of feed flow rate and motive steam flow rate of 23% and 7.3%, respectively.

Keywords: Pareto-optimization; Response surface methodology; regstats; Genetic algorithm; gamultiobj

1. Introduction

The growth in the world's population, the improving living standards, the recurrence of drought periods and the high level of water pollution of some rivers and lakes, as well as the tendency for groundwater to become increasingly brackish over time are reducing the quantity of naturally and easily accessible freshwater. At the same time, the freshwater demand is augmenting excessive. In fact, annual consumption is growing at the rate of 4%–8%, corresponding to 2.5 times the world's population increase [1]. Thus, according to Boltz [2], freshwater demands would be 40% higher than the supply in 2030, if current trends do not change.

To mitigate the effects of water scarcity, desalination became, in many arid regions, the best alternative for supplying water human habitation, agriculture, and industrial installations. In fact, according to the data published by the International Desalination Association (IDA) at the end of 2015, there are more than 18,000 desalination plants worldwide, that produce daily more than 86.5 million m^3, and this number would double in 2030 [3].

Mainly there are three desalination methods, called thermal, membrane and electrical methods. The multistage flash (MSF) desalination method is the most used in the thermic desalination industry. Jones et al. [4] reported that MSF desalination plants produce 18% of all desalinated water in the world. Unfortunately, this process consumes a large amount of thermal and electrical energy and it is, therefore, indispensable to improve continually MSF plant's design and to operate them at their optimum conditions, which reduces energy consumption, and therefore the cost of freshwater produced.

* Corresponding author.

Several studies have been conducted on the design and optimization of the MSF desalination process and interesting results have taken place. Ben Ali and Kairouani [5] used the solver 'gamultiobj' of MATLAB software, to determine the optimal values of the operating variables of a recirculation multistage flash (MSF-BR) desalting plant of 16 stages and having a nominal capacity of 26,700 m^3/d. In this optimization approach, three objectives were considered. The first is to maximize the plant's freshwater capacity. The second is to minimize the thermal energy used by the heat input section, and the third is to minimize the electric energy consumed by the main pumps of the installation. The mathematical resolution of the optimization problem has led to obtaining, for each month, a set of optimal solutions. In the second study of Ben Ali and Kairouani [6], the authors considered objective functions, the plant performance indicators, that is, the thermal performance ratio, the specific cooling water flow rate, the specific recirculating brine flow rate, and the specific feed flow rate. These parameters control the specific consumption of steam, electricity, and chemicals. The optimization results reveal that a significant improvement of the performance indicators can be obtained if optimal operating points given by solving the optimization problem are used. Harandi et al. [7] presented a new design of the MSF-BR process with two ejectors that extract secondary vapor from two successive middle stages of the heat recovery section and then used as heating steam. Optimization of this configuration called multistage flash desalination system with brine recirculation and thermal vapor compression (MSF-BR/TVC) was done using a method based on the genetic algorithm Non-dominated Sorting Genetic Algorithm (NSGA-II). Two objective functions were considered in this optimization approach. The first is to maximize the performance ratio. The second is to minimize the specific heat transfer area. Solving the optimization problem led to obtaining a Pareto front curve composed of a large number of points giving the values of the objective functions as well as the optimal values of the decision parameters. This study also showed the increase in the optimum thermal performance ratio of the plant from 9.97 to 15.27 when the number of stages of the heat recovery section increases from 17 to 27. Tanvir and Mujtaba [8] used the MINLP technique within the gPROMS model builder for optimizing the number of flash stages, and operating parameters of the MSF-BR process. During this optimization, the authors are interested in minimizing capital, utility and pumping costs of the installation, while taking into account variation in freshwater production capacity and seasonal variation of seawater temperature. Bandi et al. [9] used a differential evolution algorithm (DE) to optimize the design of three MSF process configurations. The objective function to minimize was the annual freshwater production cost. The study showed that using the DE algorithm provided a better reduction in the optimal freshwater production cost compared to optimization methods using MATLAB optimization toolbox solvers. However, the study revealed that the DE algorithm was ineffective to determine optimal values of the design parameters of MSF-once through (MSF-OT) configuration. Abduljawad and Ezzeghni [10] developed a method using a solver tool of Excel software for optimizing operating parameters of (MSF-OT) plant having 12 flash stages and a nominal production capacity of 1,200 m^3/d. The objective function to maximize was the gained output ratio at freshwater demands between 1,000 and 1,300 m^3/d. Mastro and Mistretta [11] presented an economic analysis of the MSF plant coupled to municipal solid waste (MSW) incinerator which would be used to produce brine heater steam. The study estimated the capital and operating costs of the new design and the revenues obtained from the sale of desalted water. The study showed that coupling the MSF plant with a MSW incinerator allowed using low-cost and sustainable heating steam with minimum environmental impact.

The advantages obtained by El-Dessouky et al. [12] when coupling thermal vapor compression with multi-stage flash with brine recirculation (MSF-BR/TVC), motivated us to conduct this study. Indeed, this paper presents an approach for optimization of the operating parameters of the second configuration of the MSF process, that is, once-through multistage flash desalination when coupled with thermal vapor compression, MSF-OT/TCV. In addition, this study is becoming more interesting since there are no published studies on the MSF-OT/TCV configuration.

The following sections include a description of the MSF-OT/TVC process, the approach used to optimize the operation of the installation, results obtained, and finally the conclusion.

2. Description of the MSF-OT/TVC desalination process

Fig. 1 shows a schema of a desalination plant using the MSF-OT/TVC process. The installation essentially consists of the brine heater called also heat input section, the flashing stages which are connected in series, and the steam ejector. Each flashing stage is constituted by a brine pool, vapor space, demister, condenser tubes, distillate tray, and inlet/outlet brine orifices.

The feed seawater M_f, is first screened, deaerated, chemically treated, and then it flows inside the condenser tubes of the different stages from the cold to the hot side of the plant, where it absorbs the latent heat of the condensing vapor produced in stages. Next, the feed seawater enters the heat input section, where it is heating by the heating steam, M_s. The temperature of the feed seawater then increases to a high value known as top brine temperature T_{b0} whose maximum value depends on chemicals used to prevent scale formation. The heated brine then enters the brine pool of the first flashing stage through a submerged orifice where part of this brine is flashed into water vapor. This vapor passes through a demister used to remove entrained brine droplets. This avoids contamination of the produced freshwater. Then the vapor becomes in contact with the condenser tubes (preheater), where it condenses and falls in a distillate tray. This flashing process is then repeated throughout the plant. Finally, at the last stage of the plant, the concentrated brine M_b, is discharged to the sea and the total freshwater produced M_d is collected.

The steam jet ejector uses a high-pressure motive steam M_m from a boiler to compress vapor extracted from flashing stages, M_{ev}, to the desired temperature T_s depending on the value of the top brine temperature T_{b0}. The mixture stream obtained (M_{ev} + M_m) flows to the heat input section and becomes the plant heating steam, M_s.

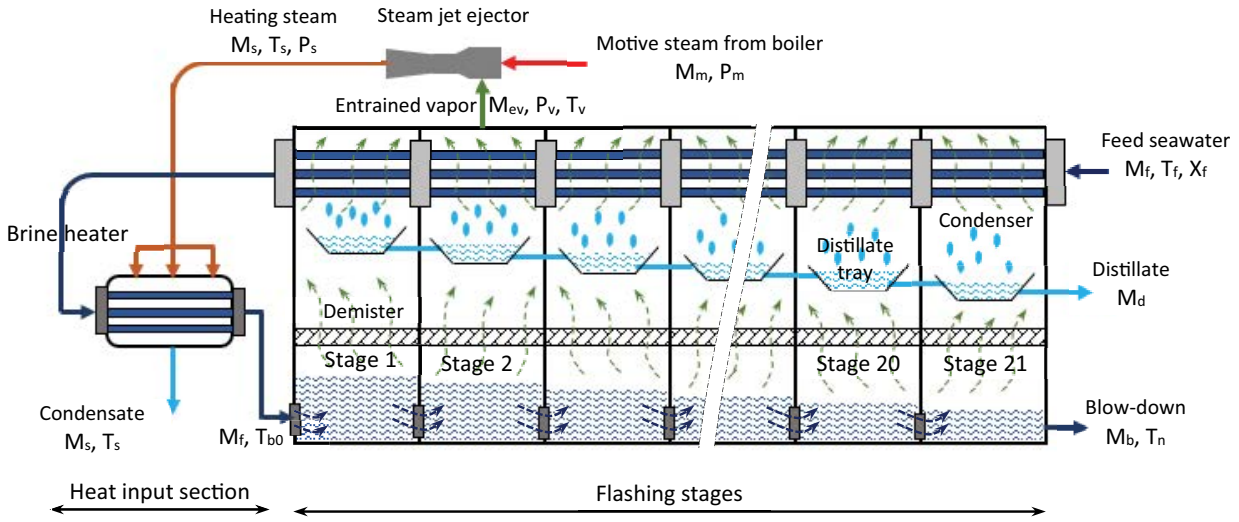

Fig. 1. Schema of the MSF-OT/TVC desalination process.

The novel configuration of the plant under consideration in this study is shown in Fig. 1. It includes 21 flashing stages and has a nominal capacity of 32,000 m^3/d. Table 1 gives the plant's characteristics [13], and those of the steam jet ejector [12] used to train vapor from the second flashing stage of the installation.

3. Optimization of operating parameters of the MSF-OT/TVC plant

3.1. Formulation of the optimization problem

The most important factors that control the operating cost of MSF-OT/TVC desalination plants are motive steam flow rate M_m, intake seawater flow rate M_f, and distillate product flow rate M_d [14].

In this work, the optimization problem is defined as follows: given the characteristics of the MSF-OT/TVC plant (Table 1), we determine optimal values of main operating parameters having a strong influence on operating cost that maximizes the distillate product flow rate and minimize the motive steam flow rate M_m and the intake seawater flow rate M_f. The operating parameters used in this optimization approach are the top brine temperature T_{b0}, and the feed seawater flows rate M_f. The adjustment of these parameters at their optimum values should reduce the rate of:

- Thermal energy consumption of the steam jet ejector;
- Electrical energy consumption of the plant main pump (feed seawater pump);
- Chemical additives consumption, which is used to control foam formation in the brine pools, and scale deposition inside the condensers and brine heater tubes.

The decision parameters (T_{b0}, M_f) for the optimization are subject to constraints defining the lower and upper values. They are determined according to the operational considerations [16]. Indeed, based on the literature review, top brine temperature T_{b0} is always maintained between 90°C and 120°C in almost all commercial MSF plants. It is recommended that T_{b0} does not exceed 120°C in order to reduce scale formation and corrosion, essentially inside the brine heater tubes. In addition, it is recommended to operate MSF plants at top brine temperature T_{b0} more than 90°C in order to avoid the low terminal temperature difference,

Table 1
Characteristics of the MSF-OT/TVC installation [12,13]

Parameter	Value
Number of stages	21
Stage width	17.660 m
Stage length	3.150 m
Stage height	4.521 m
Number of condenser tubes	1,410
Heat transfer area of condenser, A_c	3,380 m^2
Condenser tubes outer diameter	0.0445 m
Condenser tubes inner diameter	0.04197 m
Material of the condenser tubes	Cu/Ni 90/10
Density of the demister	80.317 kg/m^3
Thickness of the demister	0.200 m
Area of the demister	19.426 m^2
Number of brine heater tubes	3,800
Heat transfer area of brine heater, A_h	3,530 m^2
Brine heater tubes outer diameter	0.0244 m
Brine heater tubes inner diameter	0.0220 m
Material of brine heater tubes	Titanium
Range for the top brine temperature, T_{b0}	90°C–110°C
Temperature of reject brine, T_{bn}	40°C
Intake sea water temperature, T_f	37°C
The salinity of intake seawater, X_f	42,000 ppm
The motive steam pressure, P_m	1,500 kPa
Compression ratio for the steam jet ejector, C_r	<5

TTD (T_{vi}–T_{fi}) found mainly in the last stages. Designers of MSF plants recommend that TTD must be greater than three for stable and steady operation [15]. The limits of the feed seawater flow rate M_f are dictated by its velocity in the condensers and brine heater tubes, which should be between 1.5 and 3 m/s. The lower limit is imposed in order to not degrade the heat transfer quality at the condensers and brine heater. The upper limit is imposed in order to avoid the erosion of the brine heater and condenser tubes and higher pumping costs [16]. Therefore, we get for the MSF-OT/TVC studied, $(M_f)_{\min}$ equal to 2,900 kg/s, and $(M_f)_{\max}$ equal to 5,800 kg/s.

The optimization problem is described mathematically by:

$$\min F = \begin{cases} f_1 = -M_d\left(T_{b0}, M_f\right) \\ f_2 = M_m\left(T_{b0}, M_f\right) \\ f_3 = M_f \end{cases} \quad (1)$$

$$T_{b0},\ M_f$$

$$90 \le T_{b0}\left(^{\circ}\mathrm{C}\right) \le 120$$

$$2{,}900 \le M_f\left(\mathrm{kg/s}\right) \le 5{,}800$$

The resolution of the optimization problem required the determination previously the expressions of distillate produced flow rate M_d, and motive steam flow rate M_m as a function of the decision variables T_{b0} and M_f. For that, we used the solver 'regstats' of MATLAB software and the solver "fsolve" of MATLAB software for solving the system of equations resulting from the mathematical modeling of the MSF-OT/TVC process.

3.2. MSF-OT/TVC process model

Fig. 2 shows the steady-state model equations of the MSF-OT/TVC process considered in this study. The parameters used in these equations are shown in Figs. 1 and 3. The mathematical model is constituted of a set of mass and energy balances plus heat transfer equations of condensers and brine heater. Model equations were developed using the following assumptions:

- Salinity of distillate products is negligible.
- Condensate in the heat input section is in the saturated liquid state.
- There are no heat losses from the stages and the brine heater to the plant surroundings.
- Physical properties of the brine are variable and depend on temperature and salinity.
- Physical properties of distillate products, heating steam and flashed brine vapor are variable and depend on temperature.
- Overall heat transfer coefficients of the condensers (U_{ci}) and the brine heater (U_h) depend on:
- Flow rate, temperature, and physical proprieties of the flashed brine vapor/heating steam.
- Flow rate, temperature, and physical proprieties of the feed seawater.
- Thermal conductivity of tube material, inner and out diameter, and fouling resistance.
- Thermodynamic losses include the boiling point elevation and the non-equilibrium allowance. They depend on temperature, salinity, and flow rate of the brine and its level in the stage.

3.3. Determination of the expressions of the objective functions f_1 and f_2

In this study, we used the MATLAB solver 'regstats', which uses the response surface methodology (RSM), for approximating the objective functions f_1 and f_2, as a function of the decision variables (T_{b0}, M_f).

RSM is a statistical analysis technique widely used in the field of engineering and manufacture for modeling and analyzing multifactor systems. It allows finding an

- *Stage model*

  Mass balance in the flash chamber: $B_{i-1} = B_i + D_i$ and $X_{i-1}B_{i-1} = X_iB_i$

  Energy balance for the flashing brine: $D_i\lambda_{vi} = B_{i-1}C_{pbi-1}(T_{i-1} - T_i)$

  Energy balance for seawater in the condenser tubes:

  $$D_i\lambda_{ci} + C_{pdi}(T_{di-1} - T_{di})\sum_{k=1}^{i-1} D_k = M_fC_{pfi}\left(T_{fi} - T_{fi+1}\right)$$

  $$T_{di} = T_{vi} = T_i - NEA_i - BPE_i$$

  Heat transfer equation for the condenser: $M_fC_{pfi}\left(T_{fi} - T_{fi+1}\right) = U_iA_c(LMTD)_i$

  $$(LMTD)_i = \left(T_{fi} - T_{fi+1}\right)/ln\left[\left(T_{vi} - T_{fi+1}\right)/\left(T_{vi} - T_{fi}\right)\right]$$

- *Brine heater model*

  Energy balance for the brine in the heater: $M_fC_{ph}\left(T_{b0} - T_{f1}\right) = (M_{ev} + M_m)\lambda_{ch}$

  Heat transfer equation for the brine heater: $M_fC_{ph}\left(T_{b0} - T_{f1}\right) = U_hA_h(LMTD)_h$

  $$(LMTD)_h = (T_{b0} - t_1)/ln\left[\left(T_s - T_{f1}\right)/(T_s - T_{b0})\right]$$

- *Steam jet ejector model*

  Expression of the entrainment ratio:

  $$Ra = M_m/M_{ev} = 0{,}296\left[\left(P_s^{1.19}/P_v^{1.04}\right)(P_m/P_v)^{0.015}\right](PCF/TCF) \le 5{,}5$$

  $$PCF = 3x10^{-7}(P_m)^2 - 9x10^{-4}P_m + 1.6101$$

  $$TCF = 2x10^{-8}(T_v)^2 - 6x10^{-4}T_v + 1.0047$$

  The compression ratio Cr must satisfy the condition: $1{,}5 \le Cr = (P_s/P_v) \le 5$

Fig. 2. Steady-state MSF-OT/TVC process model.

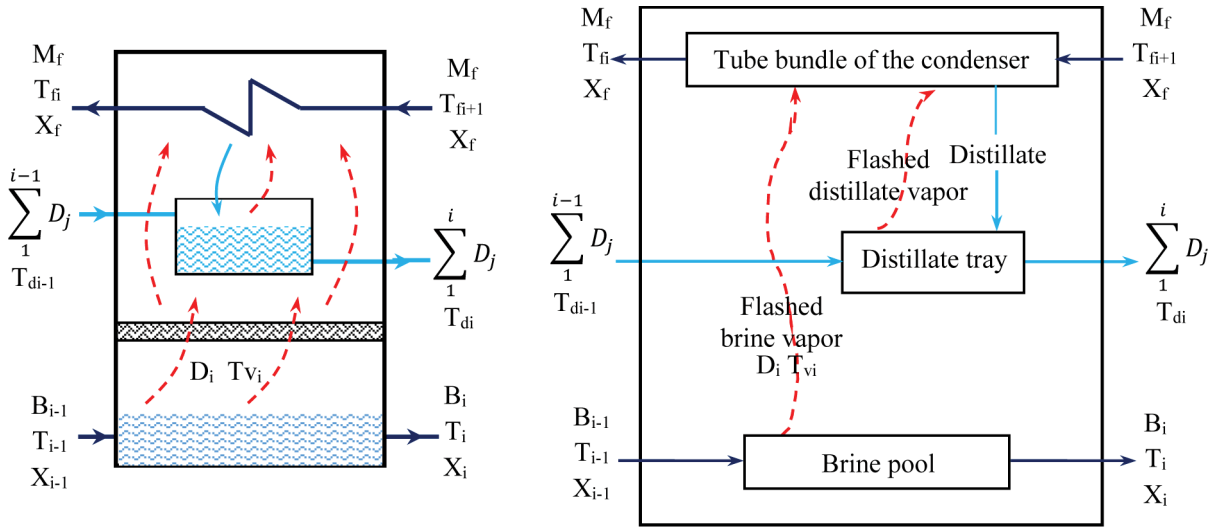

Fig. 3. Scheme of the *i*th flash chamber of the MSF-OT/TVC process.

adequate relationship between several input variables and one or more responses. Most of the time, such a relationship is unknown but can be approached by a polynomial model. In most cases, a second-degree polynomial model, with the following form, is used [17]:

$$Y = \alpha_0 + \sum_{i=1}^{k}\alpha_i X_i + \sum_{i=1}^{k}\alpha_{ii} X_i^2 + \sum_{j=2}^{k}\sum_{i=1}^{j-1}\alpha_{ij} X_i X_j \quad (2)$$

where Y is the response, α_0 is the constant term, α_1, …, α_k are the coefficients of the linear terms, α_{11}, …, α_{kk} are the coefficients of the quadratic terms, α_{12}, …, $\alpha_{(k-1)k}$ are the coefficients of the interaction parameters, and X_1, …, X_k are the coded values of the actual factors x_1, …, x_k. They are defined by the following equation:

$$X_i = \frac{x_i - \left(x_i^U + x_i^L\right)/2}{\left(x_i^U - x_i^L\right)/2} \quad (3)$$

where x_i^U and x_i^L are the upper and lower values of factor x_i. The regression coefficient values (α_i, α_{ij}, α_{ij}) of this mathematical model are estimated by using the method of least squares.

In our study two responses were considered, Y_1 corresponds to total distillate flow rate M_d, and Y_2 corresponds to heating steam flow rate M_m. The input factors were top brine temperature, T_{b0} for X_1, and feed seawater flow rate, M_f for X_2. In addition to that, we used the central composite face-centered (CCF) design to generate the predictive models for the two responses. Thus, according to the CCF design for two factors (Fig. 4), 10 different simulations have been done. These 10 simulation points included $2^2 = 4$ factorial points, $2 \times 2 = 4$ axial points, and 2 center points. Each coded factor had three levels of −1, 0, and +1. Table 2 shows the values of the independent variables for these levels. The values of the responses for each simulation had obtained by using the solver fsolve of MATLAB software for solving

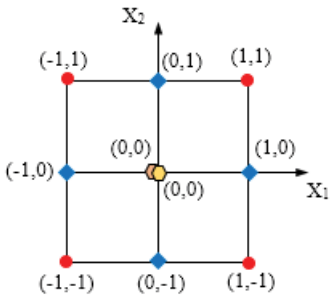

Fig. 4. Experimental points of a CCF design for two factors.

the system of equations resulting from the modeling of the MSF-OT/TVC process. The CCF design used in this study is shown in Table 3. It was analyzed by using the multilinear regression function 'regstats' of MATLAB software. The results obtained are shown in Table 4.

The coefficients of the mathematical models and their probability values have been determined using least-square regression analysis. Coefficients with a probability value <0.05 are significant; others that are insignificant have been eliminated from the models. Therefore, we obtained the following coded second-order polynomial response surface models:

$$Y_1 = M_d = 467.840 + 101.315X_1 + 155.707X_2 + 33.765X_1X_2 - 1.955X_1^2 \quad (4)$$

$$Y_2 = M_m = 28.6993 + 0.9300X_1 + 1.2983X_2 \quad (5)$$

The accuracy of the models was firstly verified using the adequacy graphs (Fig. 5) which compare the results calculated by the models with the values of the experiment plan. For both models, the points are aligned on the line $y = x$, so the descriptive quality of the models was excellent.

Table 2
Values and levels of the factors

Natural factors	Coded levels (X_1, X_2)		
	–1	0	1
T_{b0} (°C):x_1	90	105	120
M_f (Kg/s):x_2	2,900	4,350	5,800

Table 3
Coded CCF design matrix and responses

Run	Factors		Responses	
	X_1 T_{b0}	X_2 M_f	Y_1 (M_d)	Y_2 (M_m)
1	1	–1	379.02	28.28
2	–1	–1	243.64	26.54
3	0	0	468.25	28.85
4	0	1	624.24	30.14
5	1	1	757.65	30.76
6	0	0	468.25	28.85
7	0	–1	312.20	27.48
8	–1	1	487.21	29.19
9	1	0	566.51	29.34
10	–1	0	365.44	27.07

Table 4
Estimated effects for the responses Y_1 and Y_2

	Responses			
	Y_1:M_d		Y_2:M_m	
Effect	Estimate	*P*-Value	Estimate	*P*-Value
Average	467.840	0.0000	28.6993	0.0000
X_1	101.315	0.0000	0.9300	0.0011
X_2	155.707	0.0000	1.2983	0.0002
X_1X_2	33.765	0.0000	–0.0425	0.7673
X_1X_1	–1.955	0.0102	–0.3436	0.1220
X_2X_2	0.790	0.1384	0.2614	0.2110
	R^2 = 0.9999	R^2_{adj} = 0.9999	R^2 = 0.9820	R^2_{adj} = 0.9594

The quality of the models has also been verified by the application of the analysis of variance. Calculated Fisher values F_{value} of the models was 8.79×10^4 for Y_1 and 43.56 for Y_2. For both models, F_{value} was significantly higher than tabulated values $F_{(0.05,5.4)}$ which is equal to 6.26. Thus, the obtained models are considered statistically significant. The accuracy of the models was also verified using the determination coefficient (R^2) and the adjusted determination coefficient (R^2_{adj}). The values obtained by the analysis of the CCF design exceed 95%. It means that these models are fit well since they could explain more than 95% of the variation in responses Y_1, and Y_2. The normal probability plots of the residual displayed by Figs. 6 and 7 confirmed the good accuracy of the models. Indeed, for each response, the normal probability plot has the profile approximately a straight line; therefore, the residuals are normally distributed [18].

The objective functions f_1 and f_2 were thus obtained by replacing in Eqs. (4) and (5), the coded parameters X_1 and X_2, by their expressions given in Eq. (3). We obtained the following expressions in the uncoded form:

$$f_1(x_1,x_2) = 96.2205 - 1.8346x_1 + 5.535\times10^{-2}x_2 - 1.55\times10^{-3}x_1x_2 + 8.68\times10^{-3}x_1^2 \quad (6)$$

$$f_2(x_1,x_2) = 18.2944 + 0.062x_1 + 8.953\times10^{-4}x_2 \quad (7)$$

3.4. Resolution of the optimization problem

Using the results obtained in the previous section, the optimization problem was mathematically formulated as:

$$\text{Minimize } F = \begin{cases} f_1 = 96.2205 - 1.8346x_1 + 5.535\times10^{-2}x_2 - 1.55\times10^{-3}x_1x_2 + 8.68\times10^{-3}x_1^2 \\ f_2 = 18.2944 + 0.062x_1 + 8.953\times10^{-4}x_2 \\ f_3 = x_2 \end{cases} \quad (8)$$

$$90 \le x_1 \le 120$$

$$2{,}900 \le x_2 \le 5{,}800$$

The optimization problem to be solved involves three conflict objective functions, which must be optimized simultaneously. It is therefore considered as a multi-objective optimization problem with inequality constraints. In that case, it is not possible to obtain a single solution for the problem that would be optimal for the three objectives simultaneously, but it exists a set of solutions called Pareto optimal solutions, which are non-dominated with respect to each other. That means none of the three objective functions can be improved in value without degrading at least one of the other objective functions value.

Genetic algorithms (GA), which use Pareto optimality, have been widely used for solving multi-objective optimization problems in several fields [19–28]. These algorithms mimic the process of natural selection described by the concept of Darwin's theory of evolution [29]. Fig. 8 shows the flowchart of a standard genetic algorithm in a witch, an initial population of candidate solutions (called individuals or phenotypes) is randomly generated in the optimized space converge to better solutions by applying in a repetitive manner the following genetic operators: selection, crossover and mutation, until one of the stop criteria is reached. In general, the algorithm stops when a maximum number of generations is reached, or an acceptable value of the objective functions has been reached for the population of the current generation.

Several versions of genetic algorithms have been developed for solving many multi-objective optimization problems. Schaffer presented in 1984 the first GA called the Vector Evaluated Genetic Algorithms (VEGA) [25]. Goldberg and Richardson proposed in 1987 a version of GA that called the Niched Pareto Genetic Algorithm (NPGA) [30]. Srinivas and Deb developed the NSGA in 1994 [31]. Murata

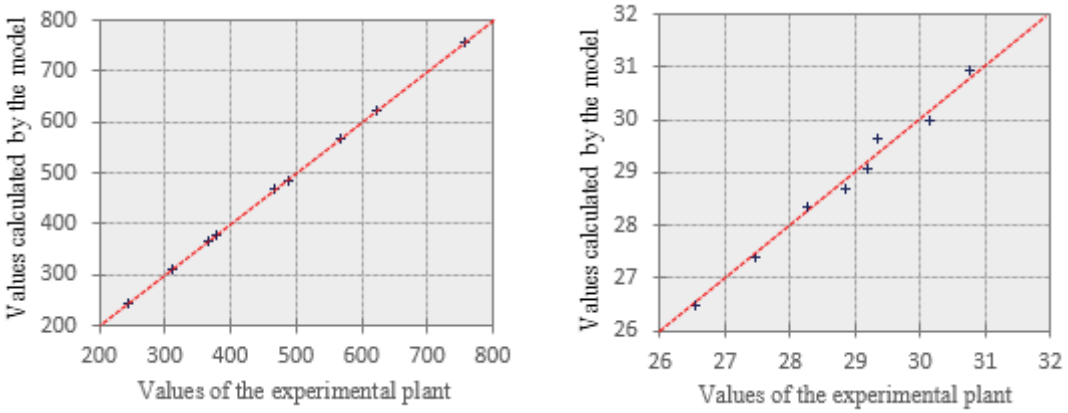

Fig. 5. Adequacy graphs of the responses Y_1 and Y_2.

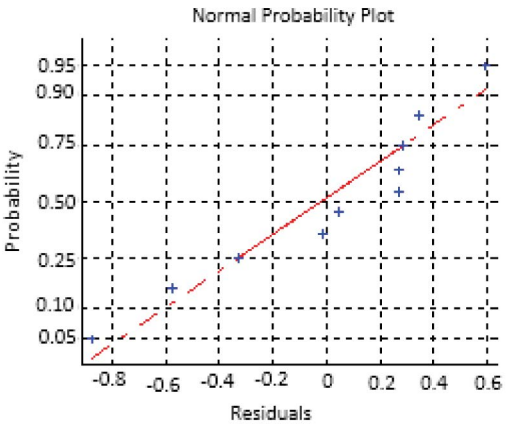

Fig. 6. Normal probability plot of response Y_1.

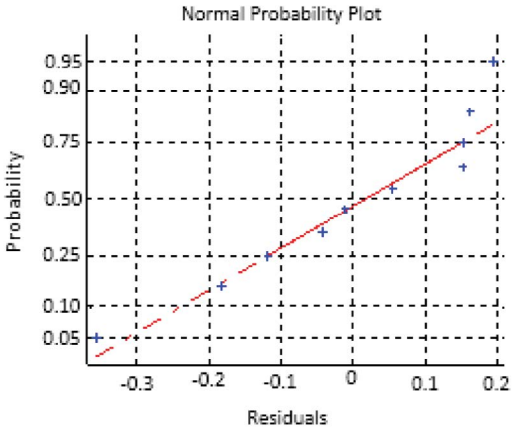

Fig. 7. Normal probability plot of response Y_2.

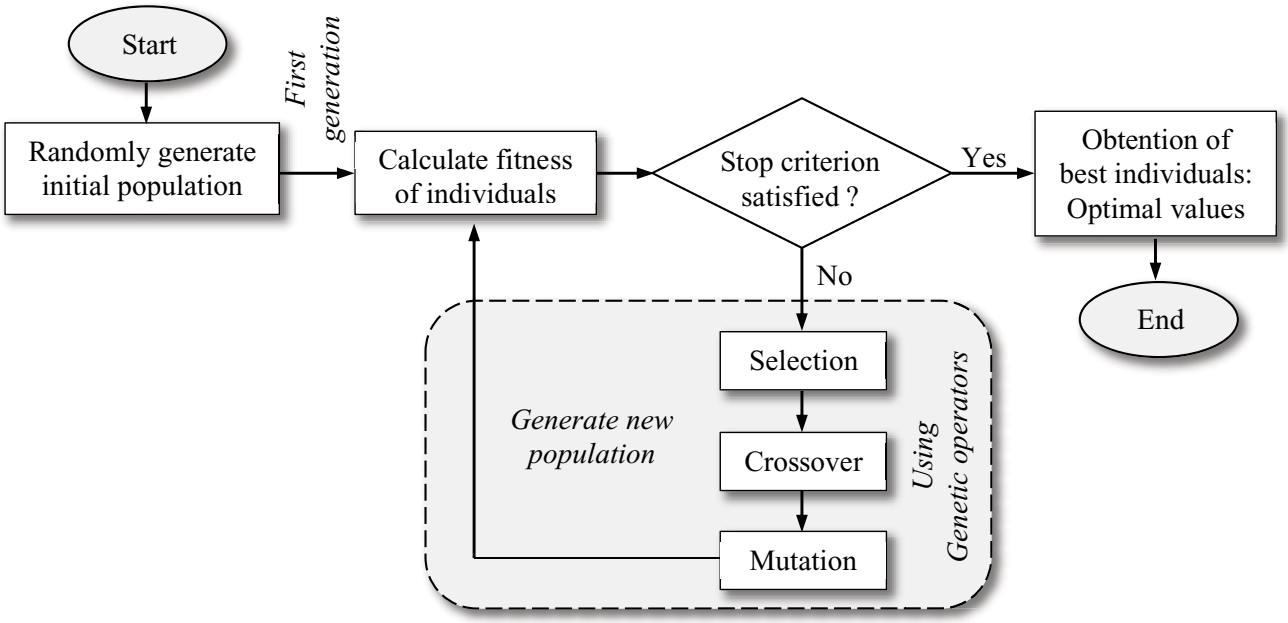

Fig. 8. Flowchart of a standard genetic algorithm.

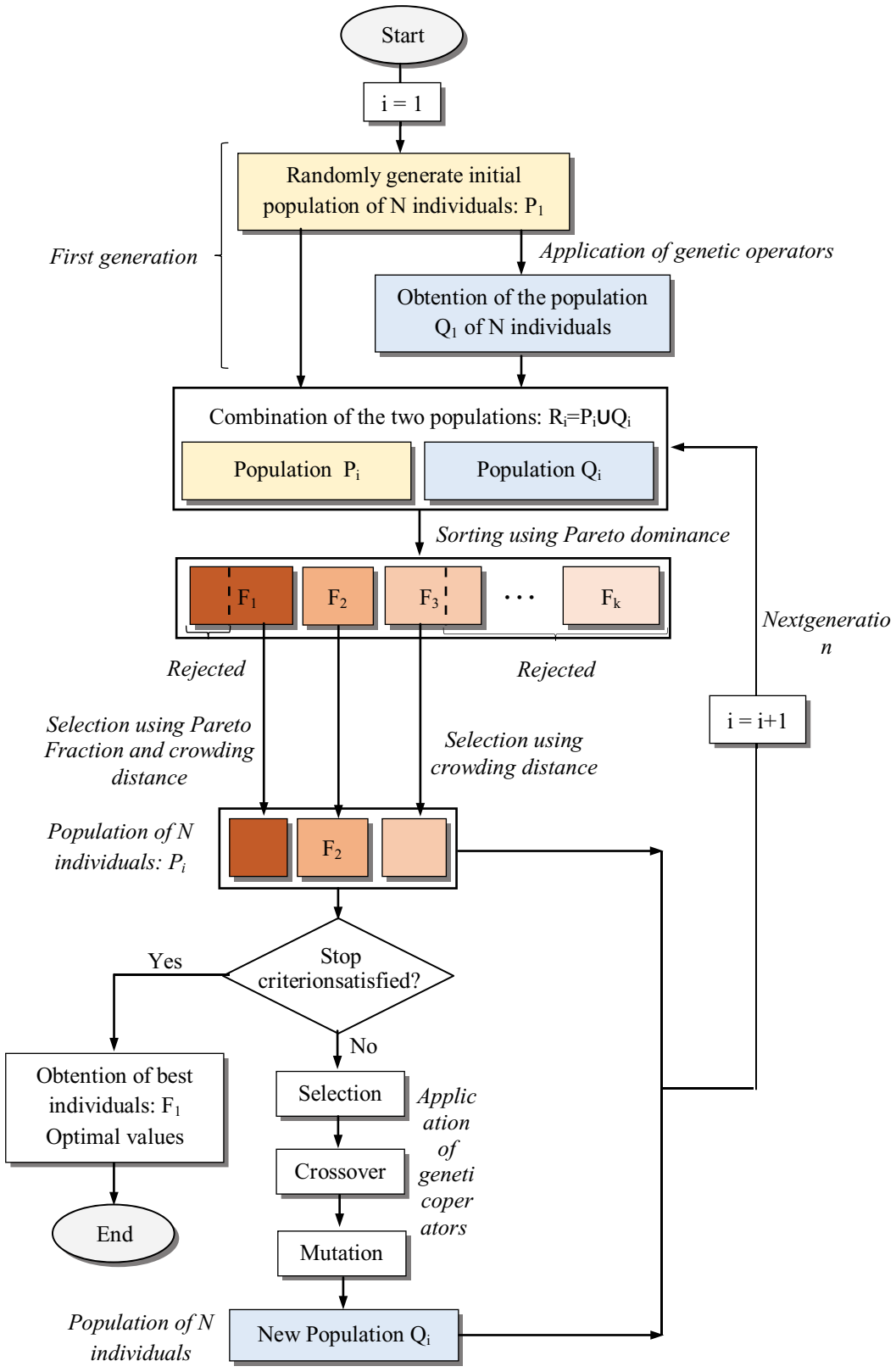

Fig. 9. Schematic of the algorithm used by the solver 'gamultiobj'.

and Ishibuchi [32] a Random Weighted Genetic Algorithm (RWGA) for solving a multi-objective optimization problem. Zitzler and Thiele [33] the Strength Pareto Evolutionary Algorithm (SPEA) as a new evolutionary algorithm for solving a multi-objective optimization problem. Knowles and Corne [34] developed three versions of a Pareto-Archived Evolution Strategy (PAES) that was used for solving multi-objective problems. Deb et al. [35] have developed a new version of the NSGA algorithm called Fast Non-dominated Sorting Genetic Algorithm (NSGA-II).

In this study, we used genetic algorithm multi-objective solver, 'gamultiobj', of MATLAB software for solving the optimization problem defined in Eq. (8). The solver uses a controlled elitist genetic algorithm (a variant of NSGA-II) for finding a Pareto front of multiple objective functions [36]. As shown in Fig. 9, the algorithm starts by randomly generating a population of N individuals constituting the first population of parents, P_1. The size of this population is defined by the parameter 'PopulationSize'. Then the usual genetic operators (selection, crossover, mutation) are applied to this population to produce the population of children Q_1 of size N. Afterwards, and at any generation i, the population P_i is combined with that Q_i to form a new population of size $2N$ called R_i. This population is classified into fronts (F_1, F_2, …, F_k) using the Pareto dominance concept. Therefore, N individuals of different non-dominance fronts fill the new population P_i, starting with the fronts with the best rank (F_1, F_2, …). In order to control the elitism and ensure population diversity for convergence to an optimal Pareto front, 'gamultiobj' uses the option 'Pareto Fraction' for specifying the fraction of individuals to maintain on the first Pareto front (F_1) in the current population P_i. The best individuals, which are less cumbersome, are chosen. The remaining individuals of the population P_{i+1} are chosen from the other fronts in the order of their ranking. The individuals of the last front that have been chosen to belong to the population P_{i+1} must also improve the population diversity. They are chosen in the descending order of their crowding distance values, which are determined by the parameter 'DistanceMeasureFcn'. Thereafter, the genetic operators (selection, crossover, and mutation) are applied to the new population P_i in order to generate a new population Q_i. These steps are repeated until a stopping criterion is satisfied. The solver 'gamultiobj' stops when the maximum number of generations is reached. This value is defined by the parameter 'Generations'. The algorithm also stops if the average change in the spread of the Pareto front over the parameter 'MaxStallGenerations' is less than the tolerance specified by the parameter 'FunctionTolerance'. Table 5 shows the values and options used in this study by 'gamultiobj' to solve the multi-objective optimization problem and thus find the optimal Pareto front.

4. Results and discussion

First, it is important to note that solving the optimization problem using 'gamultiobj' gives an optimal set of solutions for each running. This is due on the one hand to the random generation of the initial population and on the other hand to the nature of the action of genetic operators on individuals during each generation. Thus, we have as many optimal solutions as the running of the program using solver 'gamultiobj'.

Table 6 shows the results obtained after running the 'gamultiobj' solver. The algorithm stopped before reaching the maximum generation number defined by 'MaxGenerations' parameter. Fig. 10 shows the Pareto front graph, which includes the obtained Pareto-optimal solutions. These solutions represent the optimum compromise between the three objectives. A large number of optimal and diversified solutions, as shown in Fig. 11 and Table 6, have been obtained. The average distance measure of the solutions on the Pareto front was equal to 0.00784, therefore, the solutions on the Pareto front are evenly distributed.

Using the values obtained for each running (example those given in Table 6), steam cost, electricity cost, and chemical cost, plant managers can calculate the plant's operating cost for the optimal points obtained, and thus set the operating variables (T_{b0}, M_f) to the values that meet their needs economically.

The following observations are made from the results presented in Table 6:

Table 5
Values and functions used by 'gamultiobj' to solve the optimization problem

Parameter	Description	Value/function
PopulationType	Define the type of population	doubleVector
PopulationSize	Define the population size	50
SelectionFcn	Choose the function used to select parents for crossover and mutation operators	Selectiontournament
CrossoverFcn	Specify the function used to create crossover children	Crossoverintermediate
CrossoverFraction	Define the population fraction at the next generation obtained by crossover operator	0.8
MutationFcn	Define the function used for producing mutation children	Mutationadaptfeasible
ParetoFraction	Specify the fraction of individuals to keep on the first Pareto front	0.35
Generations	Define the maximum number of iterations before the algorithm stops	800
MaxStallGenerations	Define the number of successive iterations with change inferior to the value defined by FunctionTolerance	100
FunctionTolerance	Specify the geometric average of the relative change in the value of the spread generations use for stopping the running of the algorithm	10^{-6}

Table 6
Optimal values of the operating variables and objective functions

Operating variables		Objective functions			Operating variables		Objective functions		
x_1:T_{b0} (°C)	x_2:M_f (kg/s)	$-f_1$:M_d (kg/s)	f_2:M_m (kg/s)	f_3:M_f (kg/s)	x_1:T_{b0} (°C)	x_2:M_f (kg/s)	$-f_1$:M_d (kg/s)	f_2:M_m (kg/s)	f_3:M_f (kg/s)
90	2,900	242.62	26.47	2,900	115.1	5,264.5	647.79	30.14	5,264.5
93.7	3,642.8	326.94	27.36	3,642.8	106.9	3,937.7	435.60	28.45	3,937.7
119.7	5,670.2	737.62	30.79	5,670.2	116.9	4,598.9	578.40	29.66	4,598.9
110.8	3,102.3	361.55	27.94	3,102.3	101.9	4,961.0	509.99	29.05	4,961.0
105.6	5,051.3	548.26	29.36	5,051.3	116.4	5,743.6	717.85	30.65	5,743.6
102.7	3,026.9	315.06	27.37	3,026.9	97	4,454.3	423.18	28.29	4,454.3
92.4	4,064.6	356.47	27.66	4,064.6	114.5	4,178.2	510.59	29.13	4,178.2
108.7	4,396.0	498.40	28.97	4,396.0	99.3	4,230.4	417.73	28.24	4,230.4
117.3	5,366.8	678.20	30.37	5,366.8	102.7	3,804.6	395.84	28.07	3,804.6
112	5,427.1	642.00	30.09	5,427.1	113.8	4,572.7	554.06	29.44	4,572.7
112.7	3,438.5	410.72	28.36	3,438.5	118.9	4,897.2	630.75	30.05	4,897.2
109.9	4,749.8	546.75	29.36	4,749.8	101.1	3,891.3	394.96	28.04	3,891.3
120	4,989.2	650.78	30.20	4,989.2	101.4	4,286.0	435.25	28.40	4,286.0
95.9	2,901.2	270.64	26.84	2,901.2	92.2	3,344.8	291.87	27.00	3,344.8
97.6	4,699.6	450.79	28.55	4,699.6	98.2	3,135.1	304.01	27.19	3,135.1
113.2	4,128.7	495.85	29.00	4,128.7	96.3	3,385.4	317.74	27.29	3,385.4
108.9	3,614.2	410.54	28.28	3,614.2	102.9	3,039.8	317.08	27.39	3,039.8
111.1	4,865.0	568.83	29.54	4,865.0	92.9	3,663.5	323.99	27.33	3,663.5
99.9	3,313.0	330.26	27.45	3,313.0	102.8	5,622.0	585.34	29.70	5,622.0
104.5	4,505.7	481.33	28.81	4,505.7	107.8	5,297.2	592.75	29.72	5,297.2
117.7	5,106.2	648.18	30.16	5,106.2	115.8	5,744.1	713.55	30.62	5,744.1
103.7	4,666.6	492.44	28.90	4,666.6	90.6	3,235.4	273.82	26.80	3,235.4
119	4,802.2	619.46	29.97	4,802.2	100.9	5,498.0	556.40	29.47	5,498.0
110.5	4,076.5	473.27	28.79	4,076.5					

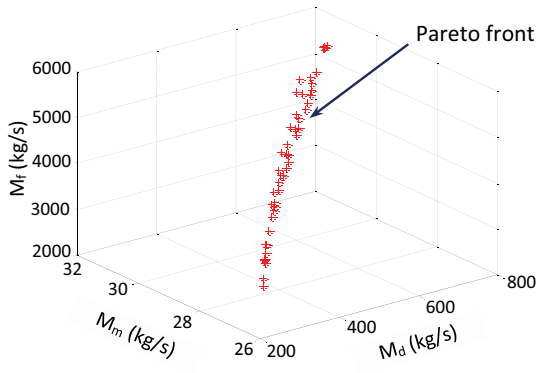

Fig. 10. Pareto-optimal solutions of the optimization problem.

- For all the optimum points, the increase in production capacity is accompanied by a simultaneous increase in the motive steam flow rate and feed flow rate, and therefore an increase in thermal and electrical energy consumption.
- Maximum value of distillate flow rate M_d (737.62 kg/s) is obtained at the point (T_{b0} = 119.7°C, M_f = 5,670.2 kg/s) corresponding to the highest value of the performance ratio PR (PR = M_d/M_m = 23.95). This parameter characterizes thermal performance of the installation.

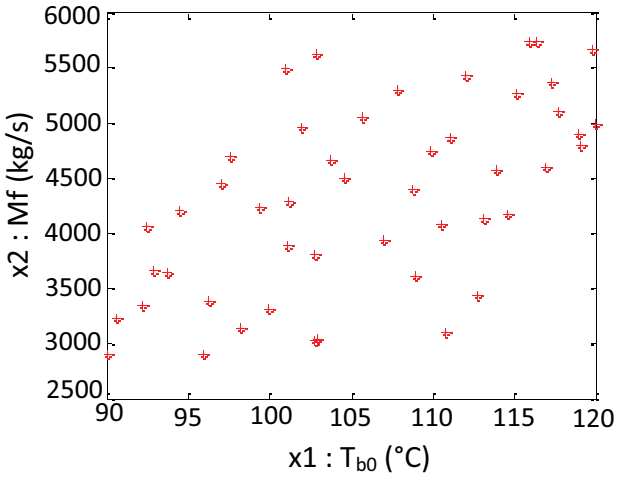

Fig. 11. Distribution of the Pareto-optimal solutions in the study space.

- Minimum value of distillate flow rate M_d (242.62 kg/s) is obtained at the point (T_{b0} = 90°C, M_f = 5,476.1 kg/s) which correspond to the lower values of the operating parameters.

Table 7
Comparison between a current operating state and optimal operating states

	Current operating state of the MSF-OT installation [4]	First optimal operating state of the MSF-OT/TVC installation		Second optimal operating state of the MSF-OT/TVC installation	
		Values of parameters	Comparison	Values of parameters	Comparison
T_{b0} (°C)	91	110.8	–	101.1	–
M_f (kg/s)	4,027	3,102.3	Gain of 23%	3,891.3	Gain of 3.4%
M_d (kg/s)	378	361.55	Reduction of 4.3%	394.96	Increase of 4.5%
M_{hs} or M_m (kg/s)	30.16	27.94	Gain of 7.3%	28.04	Gain of 7%

The above observations were valid for the results obtained during another running of the solver 'gamultiobj'.

Table 7 gives a comparison between the current operating state of the desalting installation using the MSF-OT process, which is considered as a reference configuration, and two optimal states of operation of the installation using the MSF-OT/TVC process (giving in Table 6). The first optimal state corresponds to a production capacity slightly lower than the reference configuration (reduction of 4.3%), and the second optimal state corresponds to a production capacity slightly higher than the reference configuration (an increase of 4.3%). For the first case, a significant reduction in the flow rate of feed water (23%), and on the motive steam flow rate (7.3%). This would significantly reduce the consumption of electrical energy and chemicals used, in addition to a slight reduction of the thermal energy consumed by the steam ejector. On the other hand, these advantages are accompanied by a slight reduction in the production capacity of the installation. For the second optimal case, we have a simultaneous increase in the production capacity of the plant and a reduction in the consumption of electrical energy, heat, and chemicals with acceptable values. These improvements can come on the one hand from the improvement of the procedure (use of thermal vapor compression), and on the other hand from the use of optimal values for the operating parameters.

5. Conclusion

In this paper, we present an approach of using solvers of MATLAB software for optimizing operating parameters of a novel configuration of MSF-OT desalting plant in order to have lower energy consumption and desalination costs. Two main operating parameters were chosen for optimization, that is, the top brine temperature T_{b0}, and the feed seawater flow rate M_f. Three objectives, which control the operating cost of the plant, were considered. The first objective is to maximize the freshwater production capacity of the plant. The second is to minimize the flow rate of motive steam used by the TVC unit in order to reduce the thermal energy consumption of the whole installation. The third objective is to minimize the feed seawater flow rate in order to reduce the electrical energy consumption of the plant's main pump, and chemical additives consumption. Firstly, the solver 'regstats' using RSM was used for estimating the expressions of the first and the second objective of the optimization problem. Afterward, the solver 'gamultiobj' using a genetic algorithm was used for solving the multi-objective optimization problem. The result is the obtaining of a large set of Pareto optimal solutions, which is constituted by various combinations of the optimal operating variables of a MSF-OT/TVC desalting plant. These solutions represent a compromise between the three objective functions.

It is important to mention that the proposed approach leads to obtain many combinations of optimal values of T_{b0} and M_f each time the developed program using the solver 'gamultiobj' is executed. The study concluded that designing and optimization of new desalting installation, combining of TVC unit with conventional MSF-OT process, would result in choosing of best-operating conditions resulting in a lower freshwater production cost.

Symbols

A	—	Heat transfer area, m^2
B	—	Brine mass flow rate, kg/s
C_p	—	Specific heat at constant pressure, kJ/kg K
C_r	—	Compression ratio
D	—	Flashing vapor flow rate, kg/s
F	—	Pareto front
LMTD	—	Logarithmic mean temperature difference, °C
M	—	Mass flow rate, kg/s
n	—	Number of stages
NEA	—	Non-equilibrium allowance, °C
PR	—	Thermal performance ratio
P	—	Pression, kPa
Q	—	Population of children
R	—	Combined population
R_a	—	Entrainment ratio
sM_f	—	Specific feed seawater flow rate
T	—	Temperature, °C
TVC	—	Thermal vapor compression
T_{b0}	—	Top brine temperature, °C
U	—	Overall heat transfer coefficient, W/m^2 K
X	—	Water salinity, ppm

Greek

λ	—	Latent heat of vaporization, kJ/kg

Subscripts

b	—	Brine
c	—	Condenser or condensate

d — Distillate product
ev — Entrained vapor
f — Feed
h — Brine heater
m — Motive steam
s — Steam
v — Vapor

References

[1] N. Lior, Membrane-Distillation Desalination: Status and Potential, 17th International Congress of Chemical and Process Conference, Prague, Czech Republic, August 27–31, 2006.
[2] F. Boltz, How Do We Prevent Today's Water Crisis Becoming Tomorrow's Catastrophe?, The World Economic Forum, 23 March 2017.
[3] International Desalination Association. Available at: www.idadesal.org.
[4] E. Jones, M. Qadir, M.T.H. van Vliet, V. Smakhtin, S.-m. Kang, The state of desalination and brine production: a global outlook, Sci. Total Environ., 657 (2019) 1343–1356.
[5] M. Ben Ali, L. Kairouani, Multi-objective optimization of operating parameters of a MSF-BR desalination plant using solver optimization tool of Matlab software, Desalination, 381 (2016) 71–83.
[6] M. Ben Ali, L. Kairouani, Improvement of performance indicators of multistage flash desalination plant using genetic algorithms, Water Desal. Res. J., 1 (2017) 45–55.
[7] H.B. Harandi, M. Rahnama, E.J. Javaran, A. Asadi, Performance optimization of a multi stage flash desalination unit with thermal vapor compression using genetic algorithm, Appl. Therm. Eng., 123 (2017) 1106–1119.
[8] M.S. Tanvir, I.M. Mujtaba, Optimisation of design and operation of MSF desalination process using MINLP technique in gPROMS, Desalination, 222 (2008) 419–430.
[9] C.S. Bandi, R. Uppaluri, A. Kumar, Global optimization of MSF seawater desalination processes, Desalination, 394 (2016) 30–43.
[10] M. Abduljawad, U. Ezzeghni, Optimization of Tajoura MSF desalination plant, Desalination, 254 (2010) 23–28.
[11] F.L. Mastro, M. Mistretta, Thermoeconomic analysis of a coupled municipal solid waste thermovalorization–MSF desalination plant: an Italian case study, Desalination, 196 (2006) 293–305.
[12] H. El-Dessouky, H. Ettouney, H. Al-Fulaij, F. Mandani, Multistage flash desalination combined with thermal vapor compression, Chem. Eng. Process., 39 (2000) 343–356.
[13] H. Al-Fulaija, A.B. Cipollina, D. Bogle, H. Ettouney, Once through multistage flash desalination: gPROMS dynamic and steady state modeling, Desal. Water Treat., 18 (2010) 46–60.
[14] H.T. El-Dessouky, H.M. Ettouney, Fundamentals of Salt Water Desalination, Elsevier Science Ltd., Amsterdam, 2002.
[15] E.A.M. Hawaidi, I.M. Mujtaba, Simulation and optimization of MSF desalination process for fixed freshwater demand: impact of brine heater fouling, Chem. Eng. J., 165 (2010) 545–553.
[16] A.M. El-Nashar, Optimization of operating parameters of MSF plants through automatic setpoint control, Desalination, 116 (1998) 89–107.
[17] A.I. Khuri, M. Conlon, Simultaneous optimization of multiple responses represented by polynomial regression functions, Technometrics, 23 (1981) 363–375.
[18] N. Jose, S. Sengupta, J.K. Basu, Optimization of oxidative desulfurization of thiophene using Cu/titanium silicate-1 by box-behnken design, Fuel, 90 (2011) 626–632.
[19] M.H. Khoshgoftar Manesh, M. Amidpour, Multi-objective thermoeconomic optimization of coupling MSF desalination with PWR nuclear power plant through evolutionary algorithms, Desalination, 249 (2009) 1332–1344.
[20] C.A.C. Coello, A comprehensive survey of evolutionary-based multiobjective optimization techniques, Knowl. Inf. Syst., 1 (1999) 269–308.
[21] C.A.C. Coello, An Updated Survey of Evolutionary Multi-objective Optimization Techniques: State of the Art and Future Trends, Proceedings of the 1999 Congress on Evolutionary Computation-CEC99, IEEE, Washington, DC, USA, July 6–9 1999.
[22] C.A.C. Coello, An updated survey of GA-based multiobjective optimization techniques, ACM Comput. Surv., 32 (2000) 109–143.
[23] C.M. Fonseca, P.J. Fleming, Genetic Algorithms for Multi-objective Optimization: Formulation, Discussion and Generalization, Proceedings of ICGA-93: Fifth International NEA Non-Equilibrium Allowance, Genetic Algorithms, Morgan Kaufmann, Urbana-Champaign, IL, USA, July 17–22 1993.
[24] C.M. Fonseca, P.J. Fleming, Multiobjective Genetic Algorithms, IEE Colloquium on Genetic Algorithms for Control Systems Engineering (Digest No. 1993/130), IET, London, UK, May 28 1993, p. 21.
[25] C.M. Fonseca, P.J. Fleming, Multiobjective optimization and multiple constraint handling with evolutionary algorithms. II. Application example, IEEE Trans. Syst. Man Cybern. Part A Syst. Humans, 28 (1998) 38–47.
[26] M.T. Jensen, Reducing the run-time complexity of multiobjective EAs: the NSGA-II and other algorithms, IEEE Trans. Evol. Comput., 7 (2003) 503–515.
[27] X.J. Lei, Z.K. Shi, Overview of multi-objective optimization methods, J. Syst. Eng. Electron., 15 (2004) 142–146.
[28] J.-E. Yang, M.-J. Hwang, T.-Y. Sung, Y. Jin, Application of genetic algorithm for coded variables Xi reliability allocation in nuclear power plants, Reliab. Eng. Syst. Saf., 65 (1999) 229–238.
[29] G. Tsatsaronis, Thermoeconomic analysis and optimization of energy system, Prog. Energy Combust. Sci., 19 (1993) 227–257.
[30] J. Horn, N. Nafpliotis, D.E. Goldberg, A Niched Pareto Genetic Algorithm for Multiobjective Optimization, Proceedings of the First IEEE Conference on Evolutionary Computation. IEEE World Congress on Computational Intelligence, IEEE, Orlando, FL, USA, June 27–29 1994.
[31] N. Srinivas, K. Deb, Multiobjective optimization using nondominated sorting in genetic algorithms, J. Evol. Comput. 2 (1994) 221–248.
[32] T. Murata, H. Ishibuchi, MOGA: Multi-Objective Genetic Algorithms, Proceedings of 1995 IEEE International Conference on Evolutionary Computation, IEEE, Perth, Australia, 1995, pp. 289–294.
[33] E. Zitzler, L. Thiele, Multiobjective evolutionary algorithms: a comparative case study and the strength Pareto approach, IEEE Trans. Evol. Comput., 3 (1999) 257–271.
[34] J.D. Knowles, D.W. Corne, Approximating the nondominated front using the Pareto archived evolution strategy, Evol. Comput., 8 (1999) 149–172.
[35] K. Deb, A. Pratap, S. Agarwal, T. Meyarivan, A fast and elitist multiobjective genetic algorithm: NSGA-II, IEEE Trans. Evol. Comput., 6 (2002) 182–197.
[36] Matlab Documentation. Available at: http://www.mathworks.com/help/gads/gamultiobj.html.